

Endray: Bio-inspired Solar Powered Underwater Vehicle – Part I

Aniroodh Sivaraman,¹ A. K. P. Patel

¹Graduate student: Subsea Engineering, UH, Cullen College of Engineering,
Dept. of Mechanical Engg. Houston TX 77204-4006 e-mail: aniroodh.nittrichy@gmail.com

²Assistant Professor, Dept. of Naval Arch. & Offs. Engg., AMET University, Chennai (TN) – 603112, India
e-mail: aksharpatel@ametuniv.ac.in

Abstract: An underwater vehicle is used in diverse applications ranging from oceanographic study to defense use. Underwater vehicle has basic limitations over endurance, communication, and operating depth, mostly in case of autonomous underwater vehicle (AUV). In present design study, limitation over endurance has been taken care from the concept of renewable energy source (solar power). A solar panel mounted underwater vehicle design has been studied with the concept of bio-inspired design. Ray family (Batoidea) has been chosen to study their body shape hydrodynamics. A comparative study over two types of Ray family i.e. Manta ray and Stingray has been conducted using ANSYS Fluent[®]. Underwater gliding behavior of Sting ray and Manta ray has been studied in the absence of wing motions. And corresponding comparison made for body hydrodynamics.

Keywords: underwater vehicle; endurance; renewable energy; bio-inspired design; underwater gliding

I. Introduction

History of underwater vehicle extends from a break through by a manned American submarine called "TURTLE". Starting from TURTLE submarine to present advance underwater vehicles e.g. HUGIN series, they all have limited endurance. SAUV II has solar power renewable energy source which has endurance of more than 30 days [2], [3] as it is solar powered. An autonomous underwater vehicle (AUV) is designed for self tasking but demands for continuous docking and garaging because of limited endurance. An autonomous underwater glider (AUG) has theoretically infinite endurance but they are limited to narrow range of operations. Remotely operated vehicle (ROV) is used for the greater depths and higher endurance but requires adequate tethering of vehicle. In general, an underwater vehicle has basic limitations over endurance, communication, and operating depth [4]. In present approach, concept of renewable energy source i.e. solar power has been discussed as an alternate energy source. Also an effective gliding of Ray fish is studied in calm water to understand their hydrodynamic characteristics. Streamlined shape of Ray fish wing helps for smoother gliding in a deeper sea. With the effective gliding, present vehicle design, named as Endray I and II i.e. Manta ray and Stingray design respectively, can be designed as a hybrid underwater vehicle.

II. Ray Family

The fishes that belong to the Ray family are Atlantic manta, Blunt-nose stingray, Bull-nose ray, Cow-nose ray, Ocellate stingray, Rough-tail stingray, Southern eagle ray, Spiny butterfly ray, Spotted eagle ray, Little skate, etc.[1]. Aspect ratio i.e. width to length ratio for different Ray family has shown in Table I. As per available information on different types of Ray family, Manta ray and Stingray shape is adopted in present study. Manta ray shape has more centre volume and wing span whereas Stingray shape has flat bottom with more wing area. Also Stingray shape can swim faster than the Manta ray because of their difference in body shape. Manta ray and Stingray fish plan view is shown in Figure 1 which gives clear insights on body shape.

Other Ray fish has distinct and unique advantage because of their body shape. Spotted Eagle ray has higher wing span and more center volume which would facilitate in additional void space but which can also offer higher body resistance while moving forward. Another ray fish Spiny butterfly ray, which resembles the shape of butterfly, can accommodate more solar panels but it has lesser central space for equipment/machinery to be mounted.

TABLE I. ASPECT RATIO FOR DIFFERENT TYPES OF FISHES [1]

Types of Ray/Skate	Approximate aspect ratio
Atlantic Manta	2.10
Blunt-nose Stingray	1.30
Bull-nose ray	1.90
Cow-nose ray	1.80
Ocellate Stingray	1.10
Rough-tail Stingray	1.20
Southern Eagle ray	1.70
Spiny Butterfly ray	2.00
Spotted Eagle ray	2.10
Little skate	1.20

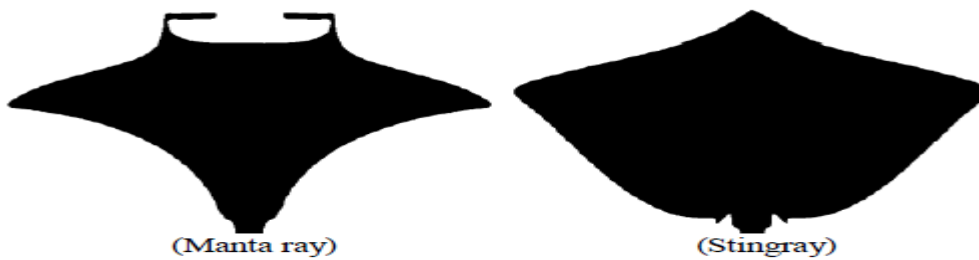


Fig. 1. Plan view of Manta ray and Stingray fish.

III. Design

This part of the paper talks about development of computer aided design (CAD) of Endray (given name of present design). In the beginning, a comparative study has been made over existing AUV designs to understand their dimensions, power requirements, endurance, etc. Table II gives the energy requirement and endurance of existing AUV designs. Table III gives the corresponding vehicle body dimensions and weight in air. In this list of different AUV vehicles, SAUV II has maximum endurance of thirty days which is solar powered whereas few vehicles have maximum endurance of around one day with overall underwater volume of displacement of 12.00 m³.

TABLE II. ENERGY REQUIREMENT AND ENDURANCE OF EXISTING AUV DESIGN

AUV Name	Energy Requirement (kWh)	Endurance (hrs)	Solar powered
HUGIN 4500	60.00	60.00	No
Bluefin 21	7.00	25.00	No
Remus 6000	11.00	8.00	No
SAUV II	2.00	720.00	Yes
Sentry	13.00	20-40	No

TABLE III. DIMESNISON AND AIR-WEIGHT OF EXISTING DESIGN

AUV Name	Dimensions (Length × Diameter) in meter	Weight in Air (Kg)
HUGIN 4500	6.0 × 1.00	1900.00
Bluefin 21	4.93 × 0.53	750.00
Remus 6000	3.99 × 0.66	240.00
SAUV II	2.30 × 1.10 × 0.50 (L × B × H)	200.00
Sentry	2.90 × 2.20 × 1.80 (L × B × H)	1250.00

A. Concept design

Endray I and Endray II are the name of the vehicles whose body shape is taken from Manta ray and Stingray fish respectively. Manta ray has design aspect ratio (B/L) of 2.10 whereas Stingray fish has design aspect ratio of around 1.20. Both designs i.e. Endray I & II is studied for the unit length ($L = 1$ meter) of vehicle to understand their body shape hydrodynamics. Top side of Ray fish has concentrated volume along the body length which is axisymmetrical. Almost 60 % of their body is in flat shape which does not contribute in available volume for equipment. For that, around the body length axis Endray is designed with regular geometry i.e. ellipsoid; to facilitate more volume along the vehicle length. And remaining body part, rigid wings of Endray, is provided with definite thickness to provide structural strength.

Bottom face of Endray is flat which provides plain surface area for solar panels. Upside down traveling of Endray is adopted to provide enough surface area to mount solar panels. Endray I has more front opening whereas Endray II has more wing area for same body volume. Fig. 2 shows the CAD drawing of Endray I and Endray II. Flow characteristics are observed in upright condition of vehicle using FluentTM. A design flow chart of present study is shown in Fig. 3. Table IV gives the principal particulars of Endray I & II design.

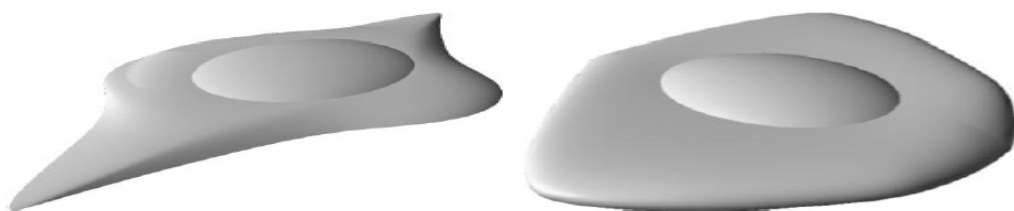


Fig. 2. CAD drawing of Endray I and Endray II.

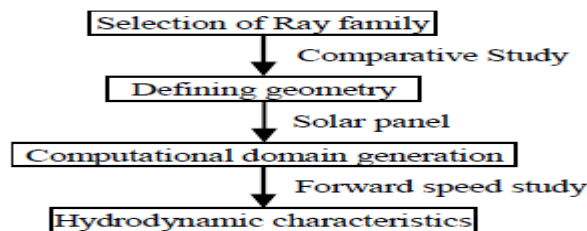


Fig. 3. Design flowchart.

TABLE IV. PRINCIPAL PARTICULARS OF ENDRAY I & II DESIGN

Vehicle name	Length (m)	Width (m)	Volume (m ³)	Bottom surface area (m ²)
Endray I	1.00	2.00	0.055	1.040
Endray II	1.00	1.20	0.050	0.820

B. Vehicle hydrodynamics

Forward motion of Endray is studied using ANSYS FluentTM at different forward speed in deep and shallow water region. Numerical solver and mesh domain details are given in Table V. A discretized domain with hexahedral mesh grid is shown in Fig. 4. A complete computational domain is shown in Fig. 5. Table VI gives the grid independence study at 3 knots for Endray I & II. A fine grid mesh is considered for the deep and shallow water study at different velocities ranging from 2 knots to 5 knots. A residual convergence study of Endray I and Endray II vehicle design for the fine grid mesh type is shown in Figs. 6 & 7 respectively at 3 knots.

TABLE V. DETAIL ON NUMERICAL SOLVER AND MESH DOMAIN

Solver name	Element type	Domain size
SST k-omega model	hexahedral	4.5L × 2L × 2L

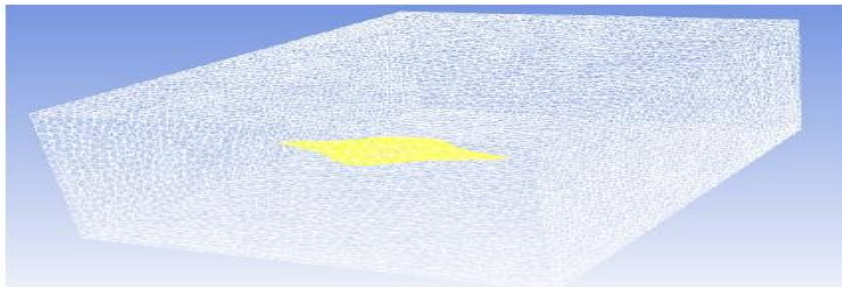


Fig. 4. Mesh domain for Endray I.

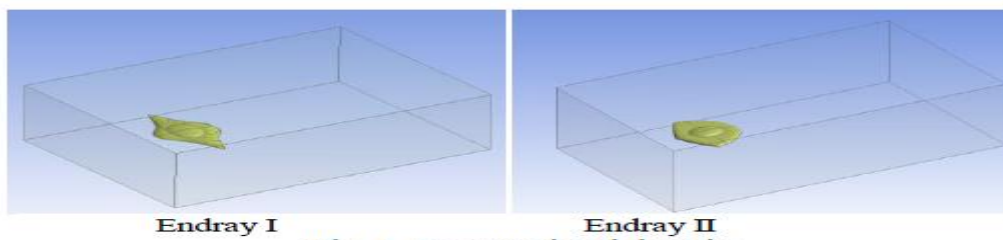


Fig. 5. Computational domain.

TABLE VI. GRID INDEPENDENCE STUDY

Grid type	No. of Elements	Drag co-efficient	Lift co-efficient
Endray I			
Coarse	270234	0.2063	2.8111×10^{-3}
Medium	301193	0.2061	2.121×10^{-3}
Fine	435980	0.2060	1.73×10^{-3}
Endray II			
Coarse	350757	0.2505	-8.15×10^{-1}
Medium	378978	0.2729	-3.5037×10^{-4}
Fine	505951	0.2784	7.5839×10^{-4}

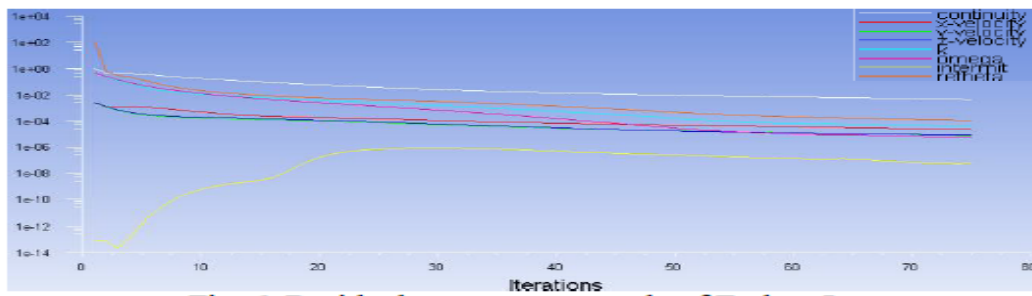


Fig. 6. Residual convergence study of Endray I.

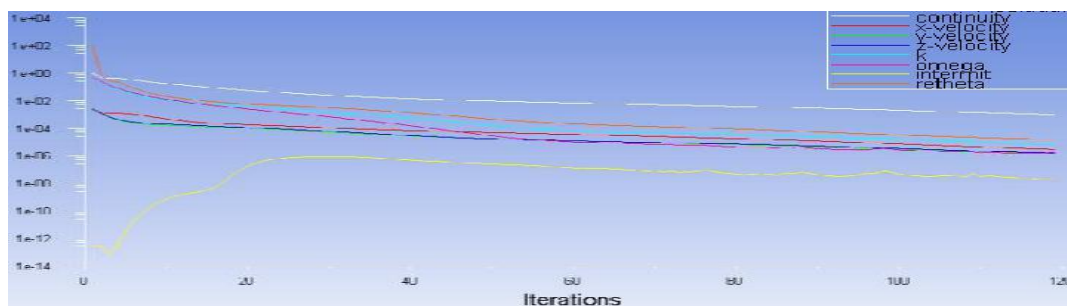


Fig. 7. Residual convergence study of Endray II.

C. Deep water study

In deep water region, side walls of the computational domain has given *slip* conditions as they represent undisturbed flow in four sides of vehicle. It is obvious that body is offering more resistance when operating at 5 knots speed which has been mentioned in Table VII. Drag co-efficient (C_D) values are derived at different forward speed which is given in Table VIII. Also same has been plotted in Fig. 8. This particular study of drag will help to understand the vehicle motion dynamics in deep water. In order to calculate the voyage time, hydrodynamic forces i.e. Lift and Drag need to be studied while vehicle moves from one location to another location.

Table VII. Resistance value for different speed

Velocity (knots)	Resistance (N)	
	Endray I	Endray II
2	916.00	1024.00
3	2004.00	2234.00
4	3516.00	3801.00
5	5428.00	5701.00

TABLE VIII. C_D VALUES AT DIFFERENT SPEED

Velocity	C_D	
	Endray I	Endray II
2 knots	0.2110	0.2873
3 knots	0.2060	0.2784
4 knots	0.2032	0.2664
5 knots	0.2008	0.2557

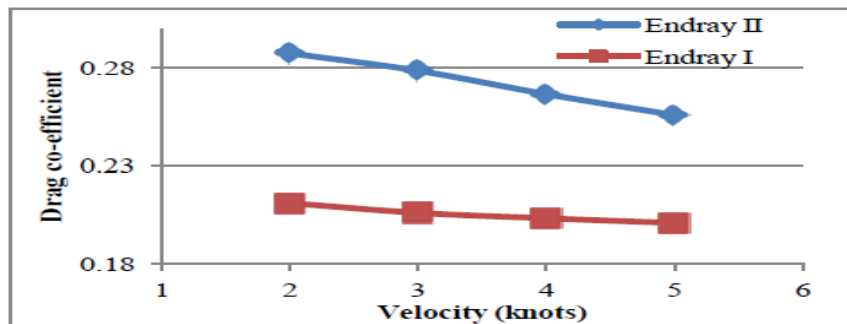


Fig. 8. Drag co-efficient value at different velocity

D. Shallow water study

In shallow water region, bottom wall of the computational domain is given *no slip* conditions. Drag and lift study at different velocity at different water depth (E) have been analyzed.

where, $E = d/L$, d is sea bed depth measured relative to vehicle position and L is vehicle length.

Drag co-efficient (C_D) values are given in Table IX,

Table X, Table XI, Table XII, Table XIII and Table XIV. This particular study of drag and lift force helps to understand vehicle motion dynamics when it is approaching the sea bed. Both Endray I and Endray II design is experiencing more resistance while moving close to seabed. It could be witnessed that near the seabed flow stream gets accelerated as the distance from the seabed decreases. As the surface velocity speed increases, this may cause increase in frictional component of resistance which contributes major part of the resistance in underwater vehicle i.e. slow speed vehicles. At higher speed of 5 knots, moving from $E = 1$ to $E = 10$, C_D value reduces almost by 20 % and 10% in case of Endray I and Endray II respectively. But there is interesting part to know about C_L and effect of angle of attack close to seabed which shall be addressed in the future study of the design.

TABLE IX. C_D AND C_L VALUES FOR E = 1

E = 1		
Velocity	C_D	
	Endray I	Endray II
3 knots	0.53629	0.5862
5 knots	1.3806	1.5049

TABLE X. C_D AND C_L VALUES FOR E = 2

E = 2		
Velocity	C_D	
	Endray I	Endray II
3 knots	0.53017	0.5864
5 knots	1.3686	1.5

TABLE XI. C_D AND C_L VALUES FOR E = 4

E = 4		
Velocity	C_D	
	Endray I	Endray II
3 knots	0.52245	0.577
5 knots	1.3457	1.4816

TABLE XII. C_D AND C_L VALUES FOR E = 6

E = 6		
Velocity	C_D	
	Endray I	Endray II
3 knots	0.5146	0.5636
5 knots	1.3242	1.4652

TABLE XIII. C_D AND C_L VALUES FOR E = 8

E = 8		
Velocity	C_D	
	Endray I	Endray II
3 knots	0.4975	0.5414
5 knots	1.2817	1.4409

TABLE XIV. C_D AND C_L VALUES FOR E = 10

E = 10		
Velocity	C_D	
	Endray I	Endray II
3 knots	0.4245	0.4986
5 knots	1.1006	1.3563

E. Power output

Solar powered vehicles are designed for better endurance when compared to conventional AUV. In this present study, Endray I and Endray II underwater vehicle design is introduced with the concept of solar powered vehicle. Table XV gives the detail about solar cell size and power (o/p) with few dealers in India. In ideal scenario, number of solar cells can be placed over the bottom face of vehicle is given in Table XVI. In real scenario, one of the possible cell arrangement, total 32 and 22 cells can be mounted over the bottom face of Endray I and Endray II respectively. In Fig. 10, right side shows the possible arrangement of solar cells on wing whereas left side of shows wing shape for Endray I and Endray II respectively. Total power output per Endray design can be calculated for given power output for one solar cell.

TABLE XV. DETAIL ON AVAILABLE SOLAR CELL

Company Name	Cell size (in mm)	Power (W)
PV Power technologies Pvt Ltd	156 x 156	4.00
EMVEE Solar	156 x 156	4.40
Tata Power Solar	156 x 156	3.11

TABLE XVI. DETAIL ON IDEAL NUMBER OF SOLAR CELL

Solar cell detail	Cell size (in mm)	Cell area (in m ²)	Available surface area (in m ²)	Ideal solar cell numbers
Endray I	156 x 156	0.025	1.1	44
Endray II	156 x 156	0.025	0.82	32

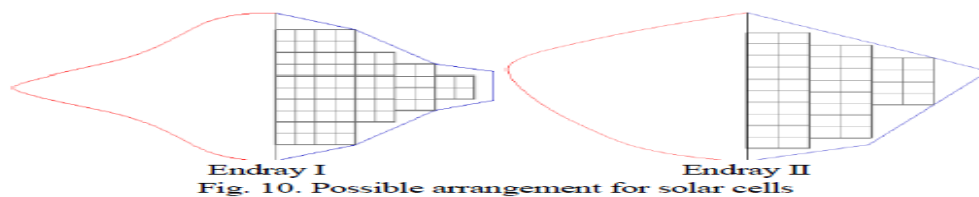


Fig. 10. Possible arrangement for solar cells

Table XVII. It has been observed for deep water region at 3 knots speed. Total power produced from each cell is mentioned for Endray design after successfully understanding the energy loss mechanism in solar cells/panels.

TABLE XVII. RESISTANCE, THRUST POWER AND POWER FROM SOLAR CELLS FOR 3 KNOTS SPEED

Parameters	Endray I	Endray II
C_D	0.2060	0.2594
Resistance (N)	532.20	550
Thrust power (W)	820.650	848.10
Power from cells (W) (Ideal power \times 0.9)	115.20	79.20

IV. Objective

It is to understand the vehicle hydrodynamics of Ray family fish shape at different operating speeds in deep and shallow water region by introducing the concept of solar powered vehicles.

V. Conclusion

- i. Manta ray and Sting ray shape has been more advantageous to understand underwater hydrodynamic characteristics
- ii. Surface area of Endray I is higher than Endray II which benefits in mounting more solar panels whereas body volume is nearly same.
- iii. In Deep water study, Endray II is offering more resistance than Endray I. This particular study of forward speed is helpful when it comes to understanding vehicle motions and control.
- iv. In Shallow water study, C_D value reduces almost by 20% and 10% in case of Endray I and Endray II respectively. This particular study of forward speed is helpful when it comes to understanding vehicle motions and control. Also to restrict the vehicle within the safe range of water depth.
- v. Endray I provides more solar cells than Endray II by 10 numbers. Total power output from each Endray design can be studied with the available power output from one solar cell under consideration of other electrical losses.
- vi. Present design approach will be extended to the next design phase where detail study on general arrangement of equipments and vehicle propulsion will be analyzed.

Acknowledgment

We acknowledge Dr. Matthew A Franchek, University of Houston for his valuable guidance and support.

Copyrights And Trademarks

*Trademark and copyright with ANSYS

References

- [1] Robert. D. love, A. Antonio Arroyo, and Eric M. Schwartz, Solar Ray: An Autonomous Solar-Powered Bio-mimetic Flapping-Wing Underwater Vehicle, Machine Intelligence Laboratory, University of Florida.
- [2] Crimmins, D. M., Patty, C. T., Beliard, M. A., Baker, J., Jalbert, J. C., Komerska, R. J., Chappell, S. G., and Blidberg, D. R., Long-Endurance Test Results of the Solar-Powered AUV System, OCEANS 2006, Boston, USA.
- [3] James Jalbert, John Baker, John Duchesney, Paul Pietryka, and William Dalton, D. R. Blidberg, Steve Chappell, Robert Nitzel, and Dr. Ken Holappa, Solar – powered Autonomous underwater vehicle, Acoustikos Div. Falmouth Scientific, Inc.
- [4] Tahadiro Hyakudome, Design of Underwater Vehicles. JAMSTEC, Japan.
- [5] Heather R. Beem and Michael S. Triantafyllou, Biomimetic Design of an Undulatory Stingray AUV Fin, Proceedings of the Twenty-second International offshore and polar Engineering Conference, Rhodes, Greece, 2012
- [6] Xiao-xu DU, Huan WANG, Cheng-zhi HAO, and Xin-liang LI, Analysis of hydrodynamic characteristics of unmanned underwater vehicle moving close to the sea bottom, Defence Technology 10, 2014, 76-81.